# Time-resolved optically stimulated luminescence of quartz in the nanosecond time domain

Christoph Schmidt, Oliver Simmank, Sebastian Kreutzer

# Time-Resolved Optically Stimulated Luminescence of Quartz in the Nanosecond Time Domain

Christoph Schmidt[a,b,*], Oliver Simmank[c], Sebastian Kreutzer[b]

[a] Chair of Geomorphology & BayCEER, University of Bayreuth, 95440 Bayreuth, Germany

[b] IRAMAT-CRP2A, UMR 5060, CNRS - Université Bordeaux Montaigne, Maison de l'Archéologie, Esplanade des Antilles, 33607 Pessac Cedex, France

[c] Freiberg Instruments GmbH, Delfter Str. 6, 09599 Freiberg, Germany

* Corresponding author: christoph.schmidt@uni-bayreuth.de

## Abstract

Time-resolved optically stimulated luminescence (TR-OSL) is one of the few methods to characterise the type of recombination centre involved in luminescence production and its response to thermal, optical and irradiation treatments. TR-OSL experiments for natural quartz yielded lifetimes mainly in the range 30–45 µs, often supplemented by shorter or longer values in the µs range. For distinct types of bedrock quartz and K-feldspar much shorter lifetimes in the ns range have been reported. Here we further explore the characteristics of this short lifetime component in quartz and look for links to specific components in the quartz OSL signal with emphasis on the slow component. Our experiments were carried out on a newly developed measurement system available as an attachment to Freiberg Instruments lexsyg research readers that allows recoding TR-OSL signals with a minimum dwell time of 2.5 ns. We demonstrate that all of the nine investigated natural quartz samples give rise to a short lifetime component in the range 30–200 ns, which does not originate from measurement artefacts or feldspar contaminants. For most samples, two further lifetimes of 0.7–3.2 µs and 39–160 µs accompany this component as indicated by multi-exponential curve fitting. Our results show that the short lifetime component does not change substantially with annealing up to 500 °C, whereas it appears to rise slightly with irradiation up to a dose of 200–800 Gy. The process behind the decrease of the short lifetime component down to ~30 ns with measurement temperature up to 110 °C could not be certainly identified. With the measurement data compiled so far, we presently cannot establish a link between the short lifetime component and the OSL slow component.

Keywords: OSL; TR-OSL; OSL lifetimes; Pulsed stimulation; Annealing; Slow component

ORCIDs:

- Christoph Schmidt: 0000-0002-2309-3209
- Sebastian Kreutzer: 0000-0002-0734-2199

Highlights

- New TR-OSL measurement system with a minimum dwell time of 2.5 ns.
- Most natural quartz samples show three lifetimes: 0.03–0.2 µs, 0.7–3.2 µs and 39–160 µs.
- The short lifetime increases with dose and decreases with measurement temperature.
- We could not find a link between the short lifetime and specific OSL components.

## 1. Introduction

The luminescence signal of quartz emitted in response to thermal (TL) or optical stimulation (OSL) is a versatile tool in environmental dosimetry as well as geoscientific and archaeological dating (e.g., [1-4]). For reliable dosimetric and dating results, it is thus of great importance to characterise the luminescence signal and associated defects of the dosimeter material as accurately as possible. Experiments including temperature scans enable investigating physical properties such as the thermal activation energy $E$ (eV) and frequency factor $s$ ($s^{-1}$) of electron traps (donor sites). The resulting bulk TL glow curve can be deconvolved into individual components, each associated with a distinct type of electron trap (e.g., [5-7]). Similarly, modulated optical stimulation reveals information about the characteristics (e.g., photoionisation cross-section) of light-sensitive electron traps in quartz (e.g., [8-10]).

However, it is more difficult to obtain information on their counterparts in the luminescence production process, the luminescence centres (acceptor sites) [11]. According to common model concepts, each type of luminescence centre occupied by a hole emits photons of characteristic energy (colour) following the capture of an electron. Specifically, this electron creates an excited state of the centre, which subsequently relaxes to a lower state or the ground state during photon emission [12-15]. Each relaxation process occurs with a distinct lifetime $\tau$ (s) that is characteristic for the centre and its specific configuration. If one or more short optical excitation pulses release trapped electrons and therefore create excited luminescence centres, the number of excited centres decays exponentially with time after stopping of stimulation [14,16].

Generally, the delay observed between stimulation and detection of OSL consists of three components: (1) the time needed to evict the electron from its trap, (2) the time it spends in the conduction band (in case of a delocalised transition) and to reach the centre, and finally (3) the relaxation time of the centre [15-18]. It is assumed that the first two contributions are much smaller (<1 ns) than the lifetime of the excited state of the centre, resulting in an expected single exponential decay of luminescence recorded after stimulation has ceased if only one type of centre is considered [15]. This view is supported by combined time-resolved OSL and exo-electron measurements which imply that the OSL lifetime detected after stopping of the stimulation is mainly dominated by the relaxation of luminescence centres [18].

Besides radiofluorescence which enables a direct look at the involved recombination sites [19,20], pulsed optical stimulation combined with time-resolved detection of luminescence (henceforth termed TR-OSL) is thus one of the few luminescence methods to obtain information about the contributing centres in response to ionising irradiation, heating or light exposure.

Numerous studies hitherto investigated luminescence lifetimes in various types of quartz as a function of different sample pre-treatments; a review is given by Chithambo et al. [21]. In essence, it was found that most quartz samples exhibit a principal lifetime component of around 30–45 µs when measured at

room temperature. This principal lifetime can be supplemented by signals with either longer (<150 µs) or shorter (several µs) lifetimes, depending on quartz formation conditions and sample history [22-27]. Remarkably, quartz extracted from crystalline rocks associated with low OSL sensitivity yielded lifetime components of about 2–4 µs, that could however not be sufficiently resolved due to the used dwell time of 2 µs [28]. In an investigation on different types of bedrock quartz, Guralnik et al. [29] presented TR-OSL lifetimes as short as 0.04 µs for some of the studied samples, which they attributed to the presence of intrinsic impurities and/or feldspar inclusions. In addition, lifetimes in the order of tens of ns were observed for time-resolved infrared stimulated luminescence (TR-IRSL) of feldspar (e.g., [15]).

TR-OSL measurements by Sanderson et al. [2018, personal communication; see also supplementary material] using 600 ps nitrogen-dye laser pulses yielded quartz lifetimes in the range <10 ns to >100 µs for a set of samples. The general reduction of lifetimes with optical and thermal pre-treatments led them to suggest a correlation between the shorter quartz lifetimes and the hard-to-bleach components in the quartz OSL signal. Specifically, they proposed a sub-conduction band recombination process being responsible for both emissions. By contrast, a clear relationship between specific OSL components and lifetimes in the µs time domain could not be established by Chithambo and Galloway [25], Chithambo [30,31] and Guralnik et al. [29], the latter studies including a documented high-purity quartz sample. In this work, we aim to further tackle the potential connection of luminescence centre relaxation lifetime and OSL signal composition with particular emphasis on short, sub-microsecond lifetimes and the hard-to-bleach (slow) component(s). This task, however, requires adequate measurement equipment capable of reliably resolving lifetime components in the $10^{-8}$–$10^{-7}$ s time domain.

The basic features of a TR-OSL stimulation and detection system relevant for discriminating luminescence lifetimes in the nanosecond range are the rise time $t_{rise}$ and fall time $t_{fall}$ of the stimulation pulse as well as the minimum dwell time of the photon counting device. Rise and fall times here refer to the time needed for the stimulation pulse to rise from 10% to 90% of maximum intensity after being switched on and to drop from 90% to 10% of maximum intensity after being switched off, respectively. Early results for lifetimes of feldspar samples were obtained using a laser system for generating stimulation pulses of 10 ns width coupled with a detection system enabling a dwell time of 5 ns [15]. Since then, most other work was carried out with LEDs as light source for pulsed stimulation. The custom-designed system formerly used by Chithambo and Galloway [32] features green (525 nm) LED stimulation and is characterised by $t_{rise}$ = 10 ns, $t_{fall}$ = 25 ns and a minimum dwell time of 5 ns; later this system was upgraded and additionally equipped with blue (470 nm) LEDs [21,25,33,34]. The commercially available system fitted to the Risø TL/OSL readers makes use of blue (470 nm) LEDs and yields $t_{rise} \approx 200$ ns, $t_{fall} \approx 100$ ns and a dwell time >0.1 ns [35]. Besides the minimum dwell time with which TR-OSL can be recorded, the main limitation for exploring short (<1 µs) lifetimes with diode-based systems are the characteristic values of $t_{rise}$ and $t_{fall}$.

In this paper, we investigate quartz OSL lifetimes <1 µs and potential links to the OSL slow component region by exploring their response to irradiation and various thermal and optical pre-treatments. The measurements were carried out on a new commercially available measurement system enabling a dwell time down to 2.5 ns. This system is used to analyse the TR-OSL signals of nine natural quartz samples, which all show a short lifetime component in the range of 100–300 ns. Finally, the implications of our experimental results are discussed.

## 2. TR-OSL experimental setup

### 2.1 Technical details of the 'fast pulsing' system

All TR-OSL measurements were conducted using a 'fast pulsing' add-on for the Freiberg Instruments *lexsyg research* luminescence reader (Fig. 1) [36]. This add-on was developed in the framework of this study and is based on 28 nm FPGA (Field Programmable Gate Array) technology supported by a dual-core ARM Cortex A9 processor. A pulse generator creates both rectangular signals that are sent to the OSL unit for sample stimulation and internal trigger pulses for recording the transient signals of the sample in response to the pulsed stimulation (Fig. 2). The internal trigger can be set to the rising or the falling edge of the pulse to record OSL during the On- and Off-time periods, respectively. The terms On-time and Off-time as used in this study refer to the cumulative time during which the stimulation source is on/off in the course of a measurement (i.e., On-time equals the On-time per pulse × the number of pulses). On- and Off-times can be adjusted as multiples of 10 ns, i.e. the main system runs with a sampling rate of 100 MHz. The (theoretical) upper limit of On- and Off-times is set to $(2^{64} – 1) \times 10$ ns. Part of the fast pulsing system, however, is operated at a sampling rate of 200 MHz and 400 MHz, allowing TR-OSL to be recorded with dwell times of 5 ns and 2.5 ns for a limited number of channels. The template memory defines the dwell time and distribution of measurement channels within the pre-selected period of signal acquisition. Typically, all channels have the same dwell time, but it is also possible to increase them logarithmically in time to record the signal at the beginning of the On- or Off-time with higher temporal resolution. The maximum number of 10 ns channels of 16,383 per recorded transient is given by the maximum number of points of the template memory, while the width of the template memory (30 bits) limits the maximum dwell time to ~10 s. To synchronise with the sampling rate of the bulk system, the deserialiser transforms the signals with 2.5 ns dwell time from the photomultiplier tube (PMT) to 10 ns dwell time by merging four channels. An adder sums up the values contained in individual channels according to the pre-defined channel length and distribution in the template memory and writes them into the data memory. Thus, the summation is done hardware-based through an FPGA before the added value is saved. The data memory itself can add together the values of up to $2^{32} – 1$ scans to generate a sum curve (On-time, Off-time or both) as output. The maximum number of count events per channel is 32,767 ($= 2^{15} – 1$) for 2.5 ns dwell time, $2^{30} – 1$ for 5 ns dwell

time and $2^{60} - 1$ for a dwell time of 10 ns and more. The PMT signal itself is carefully amplified, compared to a threshold value by the electronics and then digitally sampled. Due to the lack of any further analogue processing, the signal is not affected by dead times at all. Only the dead time resulting from the limited pulse width of the PMT has to be taken into account. If pulses are too close in time, they will be counted as one pulse. The used PMT has a pulse width (dead time) of about 10 ns, so that for an adjustable count rate of $10^7$ $s^{-1}$ the system warns the user of possible distortions due to nonlinearity of pulse counting. Finally, the output file contains a single curve representing a cumulative spectrum of radiative recombinations in the time domain.

***Fig. 1***

***Fig. 2***

Examples of stimulation pulses of different lengths are shown in Fig. 3. These were recorded by registering the light of the laser diodes directly with the PMT. For this purpose, several layers of paper, acting as 'neutral' density filter, were inserted in the filter tube to avoid oversaturation of the PMT. It can be seen that the stimulation intensity has decayed to negligible values at ~20 ns following the end of the On-time. The characteristic lifetime $\tau_{fall}$ of the falling edge of the stimulation pulse was estimated by fitting the data of the first 30 ns in the Off-time (see dashed lines in Fig. 3a) with a single exponentially decaying function (Fig. 3c). The analyses of $\tau_{fall}$ for pulse widths in the range 0.3–10 µs yielded an average value of 10 ± 1 ns.

***Fig. 3***

### 2.2 Measurement parameters

For the TR-OSL experiments, samples were stimulated with blue laser diodes (LDs) emitting at 445 nm with a maximum power density of 100 mW $cm^{-2}$ at the sample position. TR-OSL signals were detected with an EMI ET9235QB PMT through a combination of a Delta BP 365/50 EX interference filter and a 2.5 mm Hoya U340 glass filter. The resulting detection window is characterised by a transmission range from ~328 nm to ~380 nm (FWHM) and a maximum transition at 347 nm of 55%. Irradiation was performed with a $^{90}Sr/^{90}Y$ β-source with a dose rate of ~0.11 Gy $s^{-1}$ for quartz coarse grains (calibrated using Risø calibration quartz, batch 90 [37]). All measurements were carried out at room temperature (~25–30 °C inside the measurement chamber) unless indicated otherwise.

We measured and analysed only Off-time signals in this study. Most of the TR-OSL spectra presented in this study were recorded using a pulse width of 1 µs and an Off-time of 20 µs because we set the focus on the short lifetime components (<1 µs) rather than the principal lifetimes of natural quartz (~30–

45 µs) as published for instance by Chithambo and Ogundare [26] and Ankjærgaard et al. [27]. The dwell time was set to 10 ns (unless stated otherwise), the number of scans per measurement to $10^7$ and the stimulation power density to 60 mW $cm^{-2}$. This resulted in a TR-OSL measurement duration of 210 s. Furthermore, due to the finite dead time of the photon counting system of ~10 ns, TR-OSL spectra can be distorted towards photons arriving early during the Off-time period because a second photon arriving shortly after the first one during the Off-time might then not be counted (pile-up effect) [e.g., 15,32]. Therefore, we adjusted the aliquot size and stimulation power in that way that the number of detected photons was kept lower than the number of pulses in all of our experiments to allow recording of non-distorted TR-OSL spectra. The usual number of cumulative counts in the peak channel of the time-resolved spectra acquired in this study is in the order of $10^3$ or less, which translates to a probability of registering a photon of $<10^{-4}$ for each light pulse, given that $10^7$ scans were performed per spectrum. We, therefore, consider it as unlikely that our spectra are affected by pile-up effects and associated distortion of lifetimes. No preheat was applied between irradiation and TR-OSL measurement since the phosphorescence following irradiation is not correlated in time with the stimulation pulse [38].

### 2.3 Data processing

For the data processing, we utilised the statistical programming language **R** [39] and the package 'Luminescence' [40,41]. TR-OSL curves were fitted using an approach suggested by Bluscz and Adamiec [42] employing a differential evolution optimisation [43] in conjunction with nonlinear least square fitting that allows achieving a statistically justified number of OSL lifetime components in an automated procedure. For the differential evolution optimisation we used the **R** package 'DEoptim' [44,45] and for the fitting the Levenberg-Marquardt algorithm [46] as implemented in the **R** package 'minpack.lm' [47]. In a first step, start parameters were estimated optimising the function

$$\chi^2 = \sum_{j=1}^{N} w * [\frac{n_j}{c} - \sum_{i=1}^{m} A_i * e^{-\frac{t_j}{\tau_i}}]^2$$

with $n_j$ being the number of counts in the $j^{th}$ of $N$ channels, $t_j$ the corresponding Off-time, $c$ the dwell time (channel width), $A_i$ a scaling factor, $\tau_i$ the lifetime of the $i^{th}$ component and $w$ a weighing factor, which was set to

$$w = \frac{1}{\left(\frac{\sqrt{n_j}}{c}\right)^2} = \frac{c^2}{n_j}$$

assuming Poisson distribution dominated variance of the photon counts in the $j^{th}$ channel (cf. [42]). The statistical justification for adding an $m^{th}$ component was derived from an $F$-distribution ($df_1 = 2$, $df_2 = N$

– 2 * $m$ – 2 for calculating the reference values) at a significance level of 0.05. The $F$ value from the data is given by the ratio

$$F = \frac{\frac{\Delta\chi^2}{2}}{\frac{\chi^2}{N-2m-2}}$$

The so derived start parameters for $A_i$ and $\tau_i$ ($i := 1,\ldots,m$) were used as input for the final nonlinear least square fitting using the function

$$I(t) = \sum_{i=1}^{m} A_i \cdot e^{-\frac{t}{\tau_i}}$$

with $I(t)$ being the measured TR-OSL intensity. A Durbin-Watson residual statistic [48] was finally used to check for unwanted correlations between the residuals. For a fully automated lifetime estimation, the above described procedure was implemented in the **R** function `fit_OSLLifeTimes()` as part of the 'Luminescence' package version >= 0.9.0).

### 2.4 Samples and sample preparation

Nine sand-sized quartz samples from different locations in Germany, France, Jordan and Venezuela were selected for the TR-OSL experiments (see Table 1 for further details). Part of these samples shows a prominent OSL slow component which complicated their routine OSL dating. Comparative linearly modulated OSL (LM-OSL) measurements were carried out for qualitative assessment of relative contributions of fast, medium and slow components; these are shown in Figs. S1 and S2 in the supplementary material. As a benchmark, the set of samples includes a quartz reference sample (FB2A) with proven intense fast component and high luminescence sensitivity [49].

Quartz purification was carried out using routine mechanical and chemical treatments as applied in the quartz inclusion technique (e.g., [50]). An exception was sample BT1629, which was not etched in HF due to the general lack of feldspathic phases and because this sample is not used for dating purposes. All solid rock samples (BT1629, BT1647) were gently crushed in a steel mortar and sieved to the target grain size prior to chemical preparation. The lack of any contaminant phases (e.g., orthoclase, zircon) was checked by electron microprobe analyses with a JEOL JSM-6460LV Scanning Electron Microscope in high-vacuum mode (<$10^{-2}$ Pa) using a current of 20 kV. This screening of a representative number of grains per sample (e.g., 133 grains for BT729 and up to 400 grains for BT1127) demonstrated that none of the samples contained detectable amounts of feldspar (data not shown). We therefore assume that the measured TR-OSL signal does not originate from feldspar phases within the samples.

***Table 1***

## 3. Influence of the finite fall time of the stimulation pulse on measured lifetimes

Measuring accurate lifetimes in the nanosecond time domain requires a sharply defined fall-off of stimulation at the end of the optical pulse. If the characteristic fall time $\tau_{fall}$ of the stimulating light pulse is in the order of the lifetime of the signal to be measured, the measured lifetime might be distorted and longer than the 'true' lifetime [51,52]. In order to assess the impact of $\tau_{fall}$ of the used pulsing setup on the measured lifetime $\tau$, we progressively removed data channels at the beginning of the Off-time before fitting the decay curves. If there is indeed an impact of $\tau_{fall}$ (10 ± 1 ns) on the resulting lifetimes, the latter should change as a function of removed channels and attain a stable value after ~5 $\tau_{fall}$, when the stimulation light has decreased to ~1% of its initial value [52]. Such analysis for samples BT1134 and BT1385 using a 3-component-fit, however, did not reveal any trend in fitted lifetimes as a function of the number of removed data points. All three lifetime components (henceforth termed $\tau_1$, $\tau_2$ and $\tau_3$ with increasing lifetime) are identical within uncertainties for up to 10 discarded channels (data for sample BT1385 shown in Fig. S3 in the supplementary material). This can be taken as a strong indication that the detected lifetimes in the range of 100–300 ns are not significantly affected by the finite fall time of the LD stimulation.

## 4. TR-OSL spectra and associated lifetimes of quartz

### 4.1 Reproducibility of extracted lifetime components

To assess the reproducibility of the lifetime components determined by applying the fitting algorithm described in Section 2.3, we carried out five cycles of repeated β-irradiation (110 Gy) and TR-OSL measurement of one aliquot of sample BT1127. The data were fitted to three lifetime components, and we observe that all three lifetimes do not significantly change throughout the measurement sequence (within 1$\sigma$ uncertainty, except for $\tau_2$ and $\tau_3$ for cycle 2; see Fig. S4 in the supplementary material). Measurement of an empty sample cup yielded a stable Off-time TR-OSL signal about one order of magnitude lower than typical TR-OSL levels of the analysed quartz samples (Fig. S5 in the supplementary material). Therefore, we conclude that especially $\tau_1$ can be reliably extracted from the acquired TR-OSL spectra, provided that signal intensities in the initial part (<1 µs) are >5–10 cts ns$^{-1}$ above the signal corresponding to the next lifetime component and that lifetimes do not change with repeated irradiation and light exposure.

### 4.2 Lifetime components across samples

Standardised TR-OSL measurements were carried out for the samples listed in Table 1 using the measurement parameters specified in Section 2.2. For most of the samples, the natural TR-OSL signal

was very dim (<4 cts $ns^{-1}$), which complicated the reliable extraction of lifetime components from the bulk signal. Therefore, the regenerated signal following bleaching (>100 s stimulation at 445 nm and 160 °C with a power density of 16 mW $cm^{-2}$) and a β-dose of 250 Gy was recorded for two aliquots per sample and the bulk experimental data fitted to a variable number of single exponential decays (see Section 2.3). To explore a potential link between specific lifetimes and components of the quartz OSL signal (fast, medium, slow; [53,54]), a second set of two aliquots per sample was measured in the same way but with an 'optical wash' prior to TR-OSL recording to remove the fast component. This treatment consists of 100 s blue LD (445 nm) stimulation at 160 °C at a power density of ~16 mW $cm^{-2}$ (following [55]). Examples of TR-OSL spectra containing three (BT1385) and one (FB2A) lifetime components as resulting from the fitting procedure are shown in Fig. 4. This figure also depicts the signal acquisition modes of constant dwell time (Fig. 4b) and logarithmically increasing dwell time (Fig. 4a), the latter being particularly suitable for analysing lifetimes that span several orders of magnitude. Based on the routine of the **R** function `fit_OSLLifeTimes()` to find the number of components best describing the data while avoiding the problem of overfitting (see Section 2.3), three lifetime components yielded an optimised output for the majority of samples; an overview is given in Table 2 and Fig. 5.

***Fig. 4***

The results of lifetime extraction procedures demonstrate that all investigated samples show a short lifetime component ($\tau_1$) in the interval 0.07–0.25 µs, which has, to our best knowledge, only once been published for quartz before [29] and which survives optical washing (see Fig. 5b). Except for two samples (BT1629, FB2A) the values of $\tau_1$ cluster in a rather narrow range around an average of 0.18 ± 0.02 µs. The intermediate lifetime component ($\tau_2$) was present for all samples except FB2A, its values span the range 0.7–3.2 µs with an average of 2.3 ± 0.6 µs. For the longest lifetime component ($\tau_3$) the spread in values is comparatively large (39–160 µs) with an average of 79 ± 32 µs. It is remarkable that sample FB2A showed only two lifetime components without an optical wash, while $\tau_1$ disappeared following the optical wash, thus facilitating a good fit with just one exponential decay (Fig. 4b).

***Fig. 5***

The slightly increased uncertainties of lifetime components (especially $\tau_1$) following the optical wash reflect the reduced signal intensity in comparison to measurements without optical pre-treatment (Fig. 5). In general, the intermediate lifetime component ($\tau_2$) could be extracted less reliably, as indicated by a relative uncertainty of the lifetime value of ~20% compared to ~8% for both $\tau_1$ and $\tau_3$.

***Fig. 6***

*Table 2*

The scatterplot in Fig. 6 indicates that the application of an optical wash prior to TR-OSL measurement does not substantially alter the extracted lifetime components. A two-sided two-sample *t*-test shows that the difference between the lifetime components extracted in both ways is not significant ($\tau_1$: $t$ = -1,78, $df$ = 29.3, $p$ = 0.085; $\tau_2$: $t$ = -1.09, $df$ = 29.2, $p$ = 0.28; $\tau_3$: $t$ = -0.73, $df$ = 32.7, $p$ = 0.47).

The persistence of $\tau_1$ following optical treatments aimed at removing the fast OSL component (see Figs. S1 and S2 in the supplementary material) maintains the possibility that it could be associated with the slow OSL component(s), as proposed by Sanderson et al. [2018, personal communication]. The general reduction of long relaxation processes (lifetimes) following thermal and optical procedures to eliminate rapidly bleached OSL components led these authors to hypothesise on a sub-conduction band mechanism (localised transition) as a potential explanation. Such a model would, however, contradict the general view that the lifetime is mainly controlled by the relaxation process within a luminescence centre. To test this hypothesis further, we performed additional experiments trying to correlate $\tau_1$ with specific features of the OSL slow component as pointed out by Bailey [55] that are in line with the proposed model of a localised transition. In particular, for the OSL slow component, Bailey observed a positive correlation of decay rate with annealing pre-treatment and regeneration dose.

Since the other two lifetime components ($\tau_2$ and $\tau_3$) outlived the optical wash without significant change, they might equally be related to recombination processes associated with the slow OSL component(s). However, following the initial incentive of our study, we foremost focus on $\tau_1$ in subsequent analyses.

### 4.3 Annealing experiments

Bailey [55] observed an increase in the decay rate of the quartz OSL slow component after the sample had been annealed to >500 °C. Following the Zimmerman [56] model of thermal activation of luminescence centres, he explained this increased decay rate after annealing with a lower mean separation distance between donor and acceptor sites due to a larger concentration of activated luminescence centres. If there is a link between the recombination mechanism of the OSL slow component and $\tau_1$, one might expect a similar effect of annealing on the value of that lifetime component. In previous studies, no change of the principal lifetime component for annealing temperatures <500 °C was found (e.g. [30,38]), but sub-microsecond lifetimes have not yet been checked for variability with annealing treatments.

Our annealing experiments of samples BT1127, BT1385, BT1629 and BT1647 consisted of heating to temperatures of 100 °C, 200 °C, 300 °C and 500 °C with a heating rate of 5 K $s^{-1}$ and holding the temperature for 60 s before giving a β-dose of 110 Gy and measuring TR-OSL using $10^6$ pulses (other measurement parameters as specified in Section 2.2).

***Fig. 7***

Fig. 7a indicates that $\tau_1$, as obtained from fitting three lifetime components to the TR-OSL spectra, does not substantially change with annealing temperature. All values of $\tau_1$ lie between ~0.06 µs and 0.2 µs, and small variations are likely to originate from scatter-induced variations of fitting results rather than being caused by real physical effects. For sample BT1385, $\tau_1$ continuously decreased in intensity for increasing annealing temperatures, so that it could finally not be fitted anymore for an annealing temperature of 500 °C (Fig. 7a). Instead, the principal lifetime component (~45 µs) gradually sensitises throughout the measurement sequence, so that it dominates the TR-OSL signal following heating to 500 °C (Fig. 7b). Similar observations were made by Guralnik et al. [29] for one of their samples. The outlier value for sample BT1127 at an annealing temperature of 300 °C (Fig. 7a) can probably be attributed to a fitting artefact.

Changes of the principal µs-scale lifetime component in quartz with annealing temperatures >500 °C can be accounted for in the energy band model by the presence of two or more luminescent centres with distinct lifetimes each [38]. Exposure to heat leads to the transfer of holes from one centre to another, in this sense sensitising or desensitising them and entailing a shift in observed lifetime. Following that model, our experimental results would thus indicate that within the temperature range investigated here the centre responsible for $\tau_1$ is thermally stable up to 500 °C, and that it does not receive holes released from thermally less stable centres during annealing <500 °C.

### 4.4 Dependence of $\tau_1$ on regeneration dose

According to the hypothesis formulated in Section 1, a localised donor-acceptor transition should result in shorter lifetimes with increasing dose, since the average distance between electron trap and the closest luminescence centre is reduced.

To investigate the influence of the absorbed dose on $\tau_1$, we measured TR-OSL signals for samples BT1127, BT1385, BT1629 and BT1647 (two aliquots each) as a function of increasing regeneration dose in the range 50 Gy, 100 Gy, 200 Gy, 400 Gy, 800 Gy and again 50 Gy. A 'hot-bleach' for 1,800 s at 280 °C and 70 mW cm$^{-2}$ using blue LDs (445 nm) was carried out prior to each regeneration cycle to avoid carry-over of dose from previous cycles.

***Fig. 8***

Fig. 8 shows the change of $\tau_1$ with increasing regeneration dose. For doses of 50 Gy and 100 Gy, $\tau_1$ ranges between ~0.03 µs (BT1629) and ~0.13 µs (BT1127), while this lifetime component seems to be consistently shorter for sample BT1629 than for the other samples. In general, $\tau_1$ one becomes longer up to a dose of 200 Gy and then reaches a constant value of ~0.16–0.17 µs for larger doses.

From this experiment, it is however not possible to deduce a clear relationship between $\tau_1$ and absorbed dose, since the TR-OSL signal obtained from small doses (50 Gy and 100 Gy) is comparatively weak and the resulting lifetimes from the fitting procedure are susceptible to statistical scatter of the data points composing the TR-OSL decay curve. This is reflected by the increased relative uncertainty of $\tau_1$ of most samples for small regeneration doses. Hence, at this point it remains unclear whether the trend of increase in $\tau_1$ with increasing dose is a real physical effect or just a fitting artefact caused by dim signals.

### 4.5 Variation of the measurement temperature

Previous studies [23,25] revealed a strong reduction of the principal lifetime component of quartz with measurement temperature, which was attributed to the mechanism of thermal quenching. In view of the proposed direct donor-acceptor transition as recombination pathway associated with $\tau_1$, increased measurement temperature could as well foster the thermally assisted occupation of excited states within the trapping centre, from which localised recombination is more likely than from the ground state, thus decreasing the observed lifetime of this transition.

We, therefore, conducted TR-OSL measurements for samples BT1127, BT1385, BT1629 and BT1647 following a constant regeneration dose of 250 Gy, while stepwise increasing the measurement temperature in the range 25 °C, 40 °C, 50 °C, 60 °C, 70 °C, 80 °C, 90 °C, 100 °C, 110 °C. In between the regeneration cycles, we applied a hot-bleach for 1,800 s at 280 °C and 70 mW $cm^{-2}$ using blue LDs (445 nm) to prevent potential effects of accumulating dose on lifetimes throughout the measurement sequence. Due to the sharp decrease of the initial part of the resulting TR-OSL spectra, the fitting algorithm did not always sufficiently capture the first one or two data points. This means that the amplitude information contained in the fitted curve parameters is subject to considerable scatter, which unfortunately prevented the analyses of the signal intensity of $\tau_1$ as a function of measurement temperature.

***Fig. 9***

While $\tau_1$ of sample BT1629 is significantly shorter at room temperature (~25 °C) than $\tau_1$ of other samples, there is only small variation in the values of $\tau_1$ for measurement temperatures >40 °C between samples (Fig. 9a). The key finding of this experiment is that $\tau_1$ decreases in the temperature range 25–110 °C from ~0.15–0.17 µs to a seemingly stable value of ~0.03 µs. It is remarkable that the reduction of $\tau_1$ starts at much lower measurement temperatures than observed for the principal lifetime component of quartz in the range 30–40 µs, which is basically constant below measurement temperatures of 100 °C [23,25,38,57,58]. Assuming a localised donor-acceptor transition via an excited electronic state in the trap, one would expect a thermal activation mechanism following the Arrhenius law, where $\tau = 1/P \sim$

exp($W/k_BT$) with $P$ ($s^{-1}$) being the probability of activation, $W$ (eV) the activation energy, $k_B$ (eV $K^{-1}$) the Boltzmann constant and $T$ (K) the absolute temperature. Linear fits to the Arrhenius plots (Fig. 9b) have a slope $W/k_B$ and allow extracting the activation energies for samples BT1127 ($W$ = 0.18 ± 0.02 eV), BT1385 ($W$ = 0.18 ± 0.03 eV), BT1629 ($W$ = 0.08 ± 0.01 eV) and BT1647 ($W$ = 0.20 ± 0.02 eV). However, the effect of thermal quenching follows essentially the same temperature-dependence [24,59,60]; therefore, from analyses of the present dataset alone, it cannot be decided which of the two processes is involved, i.e. if the thermal activation takes place in the electron trap (speeding up the recombination process) or in the luminescence centre. It must be added though that the dataset in Fig. 9a does not allow extracting the activation energy with great confidence due to the large scatter, and interpreting these values must be done with caution.

An alternative explanation for the temperature-dependent decrease of lifetimes in quartz put forward by Chithambo and Galloway [22,23] could be the presence of shallow electron traps that cannot re-trap electrons at elevated temperatures, thus accelerating the recombination process and leading to shorter lifetimes. However, such an electron trap would produce a TL peak below room temperature.

Quite similar to the multiple-centre model explaining the variation of lifetimes with annealing (see Section 4.3), several authors have suggested that a change in the experimentally observed lifetime with measurement temperature might be caused by the presence of two luminescence centres, each with an individual characteristic lifetime [38,61]. According to this model, the different thermal quenching activation energies of the two centres lead to a temperature-dependent dominance of one of the two centres in terms of radiative transitions (Mott-Seitz mechanism). Hence, in a transitional temperature range, one of the centres increasingly determines the effective lifetime.

### 4.6 Photo-transferred thermoluminescence from the OSL slow component region

Photo-transferred thermoluminescence (PTTL) is a common observation for the OSL fast component trap, from which charge is assumed to be optically transferred through the conduction band to the trap responsible for the 110 °C peak (e.g.,[62,63]). If the recombination process associated with the OSL slow component region makes use of a sub-conduction band pathway via a localised transition, we would not expect to see PTTL in the low-temperature (<160 °C) region of the TL glow curve. To test this hypothesis, we conducted the measurement sequence shown in Table 3 to assess whether charge from the OSL slow component region induces PTTL.

***Table 3***

Additional LM-OSL measurements and deconvolution of the majority of samples proves that following an optical wash all components characterised by a photoionisation cross-section $\sigma$ in the order of $10^{-17}$–$10^{-18}$ $cm^2$ (fast and medium components) are successfully removed, while only components with $\sigma$ in

the order of $10^{-19}$–$10^{-21}$ $cm^2$ (slow components) persist (component assignment according to [9]). Details are given in the supplementary material.

As Fig. 10 shows, the depletion of these slow components causes PTTL in the glow curve region 25–160 °C with a phototransfer ratio (PTTL/OSL; [62,64]) of ~0.011 when referenced to the first 100 s of the post-OSL OSL measurement (step 4 in Table 3). While direct comparison of this value with previously determined phototransfer ratios (e.g., [62]) is hampered due to different signal integration intervals, it suggests that at least part of the signal of the slow component region results from recombination processes through the conduction band.

***Fig. 10***

## 5. Discussion

Investigation of a set of nine quartz samples from various origin and geological history showed that almost all TR-OSL curves resulting from thermally untreated samples could be best deconvolved into three lifetime components $\tau_1$ ~ 0.07–0.26 µs, $\tau_2$ ~ 0.71–2.98 µs and $\tau_3$ ~ 39–155 µs (cf. Table 2, without optical wash). A careful check for potential contaminating phases (e.g., feldspar) in the quartz samples as well as for measurement artefacts (e.g., signals from sample carriers, filter breakthrough) confirmed that the lifetimes in the order of 0.07–0.26 µs originate from quartz. Our observations are in line with OSL lifetimes in the range 0.04–2 µs found by Guralnik et al. [29] for some bedrock quartz and lifetimes in the order of 0.01–0.05 µs recorded by Sanderson et al. [2018, personal communication; see also supplementary material] for a series of quartz samples. The latter authors suspected a potential link between short quartz OSL lifetimes and a hypothesised sub-conduction band recombination process of the continuous wave (CW-)OSL slow component, based on a general reduction of lifetimes with preheating, increased stimulation temperature and erasure of rapidly bleaching CW-OSL signal components. Furthermore, Bailey [55] summarised distinct luminescence features of the OSL slow component region that clearly set it apart from the fast and medium components and fuelled again the hypothesis of a localised donor–acceptor transition which could well explain his observations. These features include an increase in the decay rate of the slow component with increasing dose and with annealing at 500 °C. Our experiments on the change of $\tau_1$ in response to annealing, increasing regeneration dose and measurement temperature aimed at testing whether we could find similar indications for the relationship between short nanosecond-scale lifetimes and the OSL slow component and its proposed recombination mechanism.

For the samples used in this study, we did not observe any substantial change of $\tau_1$ with annealing temperature up to 500 °C. Interestingly, Galloway [38] noted a decrease in the principal lifetime only if samples were heated to >600 °C. If the Zimmerman model [56] for explaining the pre-dose effect is

correct and the mechanism of direct donor-acceptor transitions would apply, $\tau_1$ should decrease with annealing due to transfer of holes from reservoir centres (R-centres) to luminescence centres and hence reduced mean separation distance between donor and acceptor. This transfer usually starts already at temperatures >400 °C [65] but should have certainly led to activation of luminescence centres following heating to 500 °C [56]. Therefore, the proposed proximity effect of donor and acceptor sites and its effect on $\tau_1$ could not be confirmed by means of the annealing experiments.

Similar to the annealing tests, the measurements of $\tau_1$ as a function of dose did not fulfil the expectations concerning the suggested localised donor-acceptor transition. Within the applied dose range (50–800 Gy), $\tau_1$ did not decrease, but instead appears to slightly increase in value up to a regeneration dose of 200 Gy, while the results for $\tau_1$ at lower doses are associated with comparatively large uncertainties. Interestingly, the idea of lifetimes that relate to the proximity of electron traps and recombination centres was formulated by Chithambo and Galloway [22] to explain the slight increase of the principal lifetime as a function of the duration of light exposure prior to TR-OSL measurement. In that way, with ongoing light exposure of the sample luminescence centres are gradually being used up, with the consequence of larger distances between trap and centre and thus also increased lifetimes. This picture, however, does not conform with our observations on the dose-dependence of $\tau_1$, where a similar effect would be expected if the proposed proximity mechanism applies.

Varying the measurement temperature demonstrated a thermally activated decrease of $\tau_1$ and Arrhenius analyses yield activation energies in the range 0.08–0.20 eV for the four measured samples. Compared to the principal lifetime of quartz (~30–45 μs), the onset of the decrease in lifetime with measurement temperature occurs at much lower temperatures for $\tau_1$ (already at or slightly above room temperature). It is nevertheless unclear whether this observation is caused by a thermally accelerated localised transition from an excited state within the electron trap, or whether it is a result of thermal quenching. Thermal quenching energies for the UV emission of natural quartz have been determined to 0.63–0.64 eV for TL [18,59], to 0.63 eV for OSL [66] and to 0.52–0.84 eV for TR-OSL [26,30,57]. The latter case would then imply that the luminescence centres producing the emissions related to either the principal lifetime or to $\tau_1$ might not be identical, or at least two different configurations of the same centre. In light of the findings from annealing and dosing experiments, however, it appears more likely that the reduction of $\tau_1$ with measurement temperature is due to thermal quenching. Another line of argumentation for explaining the shortening of lifetimes with increasing measurement temperature refers to the electron trapping sites as the relevant agent. By raising the temperature, re-trapping of delocalised electrons in shallow traps is prevented and therefore, the recombination process accelerated, resulting in shorter lifetimes [22,23].

All analyses and interpretations conducted above are based on the premise that the TR-OSL signal is a composite signal formed by a number of exponentially decaying components. While this assumption has been frequently referred to in the TR-OSL literature (e.g., [15,67,68]), to the best of our knowledge there is no experimental evidence so far that TR-OSL spectra of quartz are exclusively dominated by

the relaxation process of a luminescence centre. This should be kept in mind when trying to interpret TR-OSL spectra, and indeed alternative models to describe TR-OSL data – e.g. by stretched exponentials – were proposed [69].

Although the measurements undertaken in this study and their interpretation are not entirely conclusive, they presently cannot support the proposed association of short lifetimes, here in the range of 30–200 ns, with the quartz OSL slow component region (photoionisation cross-section: $10^{-19}$–$10^{-21}$ $cm^2$) and its suggested sub-conduction band recombination process. Since many questions on the origin of the TR-OSL signal of quartz in the nanosecond time domain and a potential link to specific OSL components remain unanswered, this study may serve as an incentive for further investigations in that field.

## 6. Conclusions

The new, commercially available TR-OSL system described and characterised in this article allowed us to study recombination processes in quartz samples in the nanosecond time domain. Along with this 'fast-pulsing' add-on, we developed a free and easy-to-use **R** function to extract luminescence lifetimes from TR-OSL spectra. The origin and exact mechanism of quartz lifetimes in the nanosecond range (30–200 ns) as obtained from the TR-OSL measurements remain unknown. All measurements conducted so far indicate that these lifetimes are not a measurement artefact nor related to impure quartz samples. The postulated association between short lifetimes, the OSL slow component region and a direct donor-acceptor transition (localised transition) could not be confirmed for the time being by measurements of the short nanosecond lifetime as a function of dose, annealing and measurement temperature, although the measurement data are not entirely conclusive. Photo-transferred TL originating from the OSL slow component region further suggests that at least one of the slow components originates from recombination pathways involving the conduction band.

## Acknowledgements

The authors are thankful to two anonymous reviewers for detailed and constructive comments. CS acknowledges a visiting scholarship by the *Initiative d'Excellence de l'université de Bordeaux* (IdEx Bordeaux) that enabled conducting the TR-OSL measurements at the IRAMAT-CRP2A in Bordeaux. Furthermore, this work was supported by a postdoc fellowship of the German Academic Exchange Service to CS (DAAD, ID 57360695). The work of SK is financed by the LabEx LaScArBx, a programme supported by the ANR (ANR-10-LABX-52). The development of the 'fast-pulsing' add-on was enabled by the project NATCH and financially supported by the Region Nouvelle-Aquitaine. The authors would like to thank Prof David Sanderson for valuable discussions on the topic and Yannick Lefrais for performing the SEM analyses. Finally, Prof Grzegorz Adamiec is thanked for detailing the differential evolution algorithm.

**References**


[1] M. Aitken, Thermoluminescence dating, Academic Press, London, 1985.

[2] M. Aitken, An introduction to optical dating. The dating of Quaternary sediments by the use of photon-stimulated luminescence, Oxford University Press, Oxford, 1998.

[3] F. Preusser, M.L. Chithambo, T. Götte, M. Martini, K. Ramseyer, E.J. Sendezera, G.J Susino, A.G. Wintle, Quartz as a natural luminescence dosimeter, Earth-Sci. Rev. 97 (2009) 184-214.

[4] I. Bailiff, E. Haskell, The Use of the Pre-Dose Technique for Environmental Dosimetry, Radiat. Prot. Dosim. 6 (1983) 245-248.

[5] R. Chen, V. Pagonis, Thermally and Optically Stimulated Luminescence - A Simulation Approach, Wiley and Sons, Chichester, 2011.

[6] S.W.S. McKeever, On the Analysis of Complex Thermoluminescence Glow-Curves: Resolution into Individual Peaks, Phys. Status Solidi (a) 62 (1980), 331-340.

[7] G. Kitis, J. Gomez-Ros, J. Tuyn, Thermoluminescence glow-curve deconvolution functions for first, second and general orders of kinetics, J. Phys. D Appl. Phys. 31 (1998) 2636-2641.

[8] E. Bulur, An alternative technique for optically stimulated luminescence (OSL) experiment, Radiat. Meas. 26 (1996) 701-709.

[9] J.S. Singarayer, R. Bailey, Further investigations of the quartz optically stimulated luminescence components using linear modulation, Radiat. Meas. 37 (2003) 451-458.

[10] G. Kitis, V. Pagonis, Computerized curve deconvolution analysis for LM-OSL, Radiat. Meas. 43 (2008) 737-741.

[11] P. Bräunlich, P. Kelly, J.-P. Fillard, Thermally Stimulated Luminescence and Conductivity, in: P. Bräunlich (Ed.), Thermally Stimulated Relaxation in Solids, Springer, Berlin/Heidelberg, 1979, pp. 35-92.

[12] M.R. Krbetschek, J. Götze, A. Dietrich, T. Trautmann, Spectral information from minerals relevant for luminescence dating, Radiat. Meas. 27 (1997) 695-748.

[13] M. Gaft, R. Reisfeld, G. Panczer, Luminescence Spectroscopy of Minerals and Materials, Springer, Berlin/Heidelberg, 2005.

[14] E.G. Yukihara, S.W.S. McKeever, Optically Stimulated Luminescence - Fundamentals and Applications, Wiley and Sons, Chichester, 2011.

[15] R. Clark, I. Bailiff, M. Tooley, A preliminary study of time-resolved luminescence in some feldspars, Radiat. Meas. 27 (1997) 211-220.

[16] M.L. Chithambo, An Introduction to Time-Resolved Optically Stimulated Luminescence, Morgan & Claypool, San Rafael, 2018.

[17] C. Ankjærgaard, M. Jain, Optically stimulated phosphorescence in quartz over the millisecond to second time scale: insights into the role of shallow traps in delaying luminescent recombination, J. Phys. D Appl. Phys. 43 (2010) 255502.

[18] S. Tsukamoto, A. Murray, C. Ankjaergaard, M. Jain, T. Lapp, Charge recombination processes in minerals studied using optically stimulated luminescence and time-resolved exo-electrons, J. Phys. D Appl. Phys. 43 (2010) 1-9.

[19] T. Schilles, N. Poolton, E. Bulur, L. Bøtter-Jensen, A.S. Murray, G. Smith, P. Riedi, G.A. Wagner, A multi-spectroscopic study of luminescence sensitivity changes in natural quartz induced by high-temperature annealing, J. Phys. D Appl. Phys. 34 (2001) 722-731.

[20] C. Schmidt, S. Kreutzer, R. DeWitt, M. Fuchs, Radiofluorescence of quartz: A review, Quat. Geochronol. 27 (2015) 66-77.

[21] M. Chithambo, C. Ankjærgaard, V. Pagonis, Time-resolved luminescence from quartz: An overview of contemporary developments and applications, Physica B 481 (2016) 8-18.

[22] M. Chithambo, R.B. Galloway, On luminescence lifetimes in quartz, Radiat. Meas. 32 (2000) 621-626.

[23] M. Chithambo, R.B. Galloway, Temperature dependence of luminescence time-resolved spectra from quartz, Radiat. Meas. 32 (2000) 627-632.

[24] I. Bailiff, Characteristics of time-resolved luminescence in quartz, Radiat. Meas. 32 (2000) 401-405.

[25] M. Chithambo, R.B. Galloway, On the slow component of luminescence stimulated from quartz by pulsed blue light-emitting diodes, Nucl. Instrum. Meth. B 183 (2001) 358-368.

[26] M. Chithambo, F. Ogundare, Luminescence lifetime components in quartz: Influence of irradiation and annealing, Radiat. Meas. 44 (2009) 453-457.

[27] C. Ankjærgaard, M. Jain, K. Thomsen, K., A.S. Murray, Optimising the separation of quartz and feldspar optically stimulated luminescence using pulsed excitation, Radiat. Meas. 45 (2010) 778-785.

[28] M. Chithambo, F. Preusser, K. Ramseyer, F. Ogundare, Time-resolved luminescence of low sensitivity quartz from crystalline rocks, Radiat. Meas. 42 (2008) 205-212.

[29] B. Guralnik, C. Ankjærgaard, M. Jain, A.S. Murray, A. Müller, M. Wälle, S.E. Lowick, F. Preusser, E.J. Rhodes, T.-S. Wu, G. Mathew, F. Herman, OSL-thermochronometry using bedrock quartz: A note of caution. Quaternary Geochronology 25 (2015) 37-48

[30] M. Chithambo, The influence of annealing and partial bleaching on luminescence lifetimes in quartz, Radiat. Meas. 37 (2003) 467-472.

[31] M. Chithambo, Dependence of the thermal influence on luminescence lifetimes from quartz on the duration of optical stimulation, Radiat. Meas. 37 (2003) 167-175.

[32] M. Chithambo, R.B. Galloway, A pulsed light-emitting-diode system for stimulation of luminescence. Meas. Sci. Technol. 11 (2000) 418-424.

[33] M.L. Chithambo, A time-correlated photon counting system for measurement of pulsed optically stimulated luminescence, J. Lumin, 131 (2011) 92-98.

[34] R.B. Galloway, Comparison of luminescence lifetimes in quartz following alpha and beta irradiation. Radiat. Meas. 35 (2002) 591-593.

[35] T. Lapp, M. Jain, C. Ankjærgaard, L. Pirtzel, Development of pulsed stimulation and Photon Timer attachments to the Risø TL/OSL reader, Radiat. Meas. 44 (2009) 571-575.

[36] D. Richter, A. Richter, K. Dornich, Lexsyg - A new system for luminescence research, Geochronometria 40 (2013) 220-228.

[37] V. Hansen, A.S. Murray, J.-P. Buylaert, E.-Y. Yeo, K. Thomsen, A new irradiated quartz for beta source calibration, Radiat. Meas. 11 (2015) 123-127.

[38] R.B. Galloway, Luminescence lifetimes in quartz: dependence on annealing temperature prior to beta irradiation. Radiat. Meas. 35 (2002) 67-77.

[39] R Core Team, A Language and Environment for Statistical Computing, R Foundation for Statistical Computing, Vienna, 2012. http://www.R-project.org/.

[40] S. Kreutzer, C. Schmidt, M.C. Fuchs, M. Dietze, M. Fischer, M. Fuchs, Introducing an R package for luminescence dating analysis, Ancient TL 30 (2012) 1-8.

[41] S. Kreutzer, C. Burow, M. Dietze, M.C. Fuchs, C. Schmidt, M. Fischer, J. Friedrich, Luminescence: Comprehensive Luminescence Dating Data Analysis. R package version 0.8.5, 2018, https://CRAN.R-project.org/package=Luminescence

[42] A. Bluszcz, G. Adamiec, Application of differential evolution to fitting OSL decay curves, Radiat. Meas. 41 (2006) 886-891.

[43] K.V. Price, R.M. Storn, J.A. Lampinen, Differential Evolution - A Practical Approach to Global Optimization, Springer, Berlin/Heidelberg, 2006.

[44] K. Mullen, D. Ardia, D. Gil, D. Windover, J. Cline, 'DEoptim': An R Package for Global Optimization by Differential Evolution, J. Stat. Softw. 40 (2016) 1-26.

[45] D. Ardia, K.M. Mullen, B.G. Peterson, J. Ulrich, 'DEoptim': Differential Evolution in 'R'. R package version 2.2-4, 2016, https://CRAN.R-project.org/package=DEoptim

[46] J.J. Moré, The Levenberg-Marquardt algorithm: Implementation and theory, in: Numerical Analysis, Springer, Berlin/Heidelberg, 1978: pp. 105-116.

[47] T.V. Elzhov, K.M. Mullen, A-N. Spiess, B. Bolker, minpack.lm: R Interface to the Levenberg-Marquardt Nonlinear Least-Squares Algorithm Found in MINPACK, Plus Support for Bounds. R package version 1.2-1, 2016, https://CRAN.R-project.org/package=minpack.lm

[48] J. Durbin, G.S. Watson, Testing for Serial Correlation in Least Squares Regression: I, Biometrika 37 (1950) 409-421.

[49] S. Kreutzer, J. Friedrich, D.C.W. Sanderson, G. Adamiec, A. Chruścińska, M. Fasoli, M. Martini, G.S. Polymeris, C.I. Burbidge, C. Schmidt, Les sables de Fontainebleau: A Natural Quartz Reference Sample and its Characterisation, Ancient TL 35 (2017) 21-31.

[50] S. Kreutzer, M. Fuchs, S. Meszner, D. Faust, OSL chronostratigraphy of a loess-palaeosol sequence in Saxony/Germany using quartz of different grain sizes, Quat. Geochronol. 10 (2012) 102-109.

[51] L.A. Shaver, L.J. Cline Love, Accuracy of Graphical Slope Method versus Deconvolution for the Evaluation of Luminescent Lifetimes Using Various Pulsed Sources. Appl. Spectrosc. 29 (1975) 485-489.

[52] H. Nagel, C. Berge, A.G. Aberle, Generalized analysis of quasi-steady-state and quasi-transient measurements of carrier lifetimes in semiconductors. J. Appl. Phys. 86 (1999) 6218-6221.

[53] R. Bailey, B.W. Smith, E.J. Rhodes, Partial bleaching and the decay form characteristics of quartz OSL, Radiat. Meas. 27 (1997) 123-136.

[54] M. Jain, A.S. Murray, L. Bøtter-Jensen, Characterisation of blue-light stimulated luminescence components in different quartz samples: implications for dose measurement, Radiat. Meas. 37 (2003) 441-449.

[55] R. Bailey, The slow component of quartz optically stimulated luminescence. Radiat. Meas. 32 (2000) 233-246.

[56] J. Zimmerman, The radiation-induced increase of the 100°C thermoluminescence sensitivity of fired quartz, J. Phys. C Solid State 4 (1971) 3265-3276.

[57] M. Chithambo, Time-resolved luminescence from annealed synthetic quartz under 525 nm pulsed green light stimulation, Radiat. Meas. 38 (2004) 553-555.

[58] M. Chithambo, F. Ogundare, Relative features of the principal and secondary luminescence lifetimes in quartz, Phys. Status Solidi C 4 (2007) 914-917.

[59] A.G. Wintle, Thermal quenching of thermoluminescence in quartz, Geophys. J. Roy. Astr. S. 41 (1975) 107-113.

[60] R. Chen, S.W.S. McKeever, Theory of Thermoluminescence and Related Phenomena, World Scientific, Singapore, 1997.

[61] V. Pagonis, M. Chithambo, R. Chen, A. Chruścińska, M. Fasoli, S.H. Li, M. Martini, K. Ramseyer, Thermal dependence of luminescence lifetimes and radioluminescence in quartz, J. Lumin. 145 (2014) 38-48.

[62] A.G. Wintle, A.S. Murray, The relationship between quartz thermoluminescence, photo-transferred thermoluminescence, and optically stimulated luminescence, Radiat. Meas. 27 (1997) 611-624.

[63] R. Bailey, Towards a general kinetic model for optically and thermally stimulated luminescence of quartz, Radiat. Meas. 33 (2001) 17-45.

[64] R. Bailey, Paper I—simulation of dose absorption in quartz over geological timescales and its implications for the precision and accuracy of optical dating, Radiat. Meas. 38 (2004) 299-310.

[65] J. Friedrich, V. Pagonis, R. Chen, S. Kreutzer, C. Schmidt, Quartz radiofluorescence: a modelling approach, J. Lumin. 186 (2017) 318-325.

[66] G.A.T. Duller, L. Boetter-Jensen, N.R.J. Poolton, Stimulation of mineral-specific luminescence from multi-mineral samples, Radiat. Meas. 24 (1995) 87-93.

[67] M. Chithambo, The analysis of time-resolved optically stimulated luminescence: II. Computer simulations and experimental results, J. Phys. D Appl. Phys. 40 (2007) 1880-1889.

[68] V. Pagonis, C. Ankjærgaard, A.S. Murray, M. Jain, R. Chen, J. Lawless, S. Greilich, Modelling the thermal quenching mechanism in quartz based on time-resolved optically stimulated luminescence, J. Lumin. 130 (2010) 902-909.

[69] M. Chithambo, Towards models for analysis of time-resolved luminescence spectra from quartz, Appl. Radiat. Isotopes 62 (2005) 941-942.

[70] T. Kolb, M. Fuchs, L. Zöller, Deciphering fluvial landscape evolution by luminescence dating of river terrace formation: a case study from Northern Bavaria, Germany, Z. Geomorphol. Supp. 60 (2016) 29-48.

[71] S. Kreutzer, M. Duval, M. Bartz, P. Bertran, M. Bosq, F. Eynaud, F. Verdin, N. Mercier, Deciphering long-term coastal dynamics using IR-RF and ESR dating: a case study from Médoc, south-west France, Quat. Geochronol. 48 (2018) 108-120.

**Table and Figure captions**

**Table 1**

List of quartz samples used for the TR-OSL experiments.

**Table 2**

Summary of lifetimes obtained for the set of samples following a regenerative β-dose of 250 Gy and either no further optical pre-treatment ('without optical wash') or with an optical wash prior to TR-OSL measurement consisting of exposure to blue LDs (445 nm) at 160 °C for 100 s at a power density of 16 mW $cm^{-2}$. Two aliquots per sample were measured and the lifetimes were extracted using the `fit_OSLLifeTimes()` function of the **R** package 'Luminescence' (v0.9.0; upcoming version). Uncertainties are quoted at 1σ.

**Table 3**

Sequence of measurements to record PTTL induced by the OSL slow component region.

**Fig. 1**

Schematic diagram showing the integration of the pulsed OSL unit into the *lexsyg research* system.

**Fig. 2**

Overview scheme showing the interaction of the system components for pulse generation and processing of TR-OSL data. Individual components are independent and self-developed functional blocks within the FPGA technology.

**Fig. 3**

The shape of stimulation pulses for pulse widths of (a) 0.3 µs and (b) 10 µs. The light emitted from the laser diodes (LDs, 445 nm) during the pulse was directly recorded with the PMT using several layers of paper for attenuating the stimulation light. The decreasing intensity during the On-time in (b) is most likely an artefact caused by pile-up effects resulting from the finite dead time of the PMT (10 ns) so that photons arriving later in the On-time are counted with a lower probability. (c) The data points for the falling edge of one pulse (in between the dashed lines in (a)) were plotted on a log scale and fitted with a linear function to estimate the 'lifetime' $\tau_{fall}$ of the stimulating signal after switching off the LDs.

**Fig. 4**

Lifetime component extraction for sample BT1385 (a; three components) and sample FB2A (b) which could be fitted to only one component following an optical wash before TR-OSL measurement (see main text for further details). The two graphs also exemplify the signal acquisition modes of constant

dwell time (b) and logarithmically increasing dwell time along the Off-time axis (a). The varying dwell times in the latter case necessitate normalisation of the intensity values per channel (to counts $s^{-1}$) to prevent distortion of the TR-OSL spectrum. To facilitate comparability, also the spectrum shown in (b) was normalised. The fitting residuals are shown in the small lower plot areas and are denoted by ε.

**Fig. 5**

Summary of lifetimes obtained from fitting three components (except for FB2A: one/two components) to TR-OSL data of all samples listed in Table 1. (a) shows lifetimes obtained following 250 Gy β-irradiation without any optical pre-treatment, while (b) displays lifetimes after an optical wash consisting of 100 s blue stimulation (445 nm) at 160 °C and at a power density of 16 mW $cm^{-2}$ (following [49]) prior to TR-OSL measurements.

**Fig. 6**

Scatterplot of three extracted lifetime components $\tau_1$ (a), $\tau_2$ (b) and $\tau_3$ (c), where the values obtained without optical pre-treatments are contrasted with values measured following an optical wash to eliminate rapidly bleachable OSL signal components. For further details, see main text.

**Fig. 7**

(a) Plot of $\tau_1$ against annealing temperature. The large value of $\tau_1$ for sample BT1127 at an annealing temperature of 300 °C is most likely a fitting artefact. (b) TR-OSL spectra of sample BT1385 following annealing to 100 °C and 500 °C.

**Fig. 8**

Lifetime $\tau_1$ as a function of regeneration dose. Each data point represents the average of two aliquots, the error bars indicate the standard deviation. Data points for individual samples are plotted with a slight offset on the dose axis to improve visualisation of error bars.

**Fig. 9**

(a) Lifetime $\tau_1$ as a function of TR-OSL measurement temperature. Each data point represents the average of two measured aliquots, the error bar depicts the standard deviation. For better graphical visualisation, data points are slightly offset against each other on the temperature axis. (b) Plot of $\ln(\tau_1)$ vs. $1/T$, where the slope is $W/k_B$. The error in $W$ reflects the standard error on the fitted slope as returned by the fitting routine; $R^2$ values for all four samples range between 0.91 and 0.95.

**Fig. 10**

Photo-transferred TL (PTTL) plotted against the OSL signal following an optical wash (as specified in the main text). The post-OSL OSL signal refers to the integrated number of counts in the first 100 s of

the OSL readout to deplete the slow component region (step 4 in Table 3). The data represents three aliquots each from samples BT729, BT992, BT1127, BT1134, BT1385, BT1629, BT1647 and FB2A, and is fitted with a linear function.

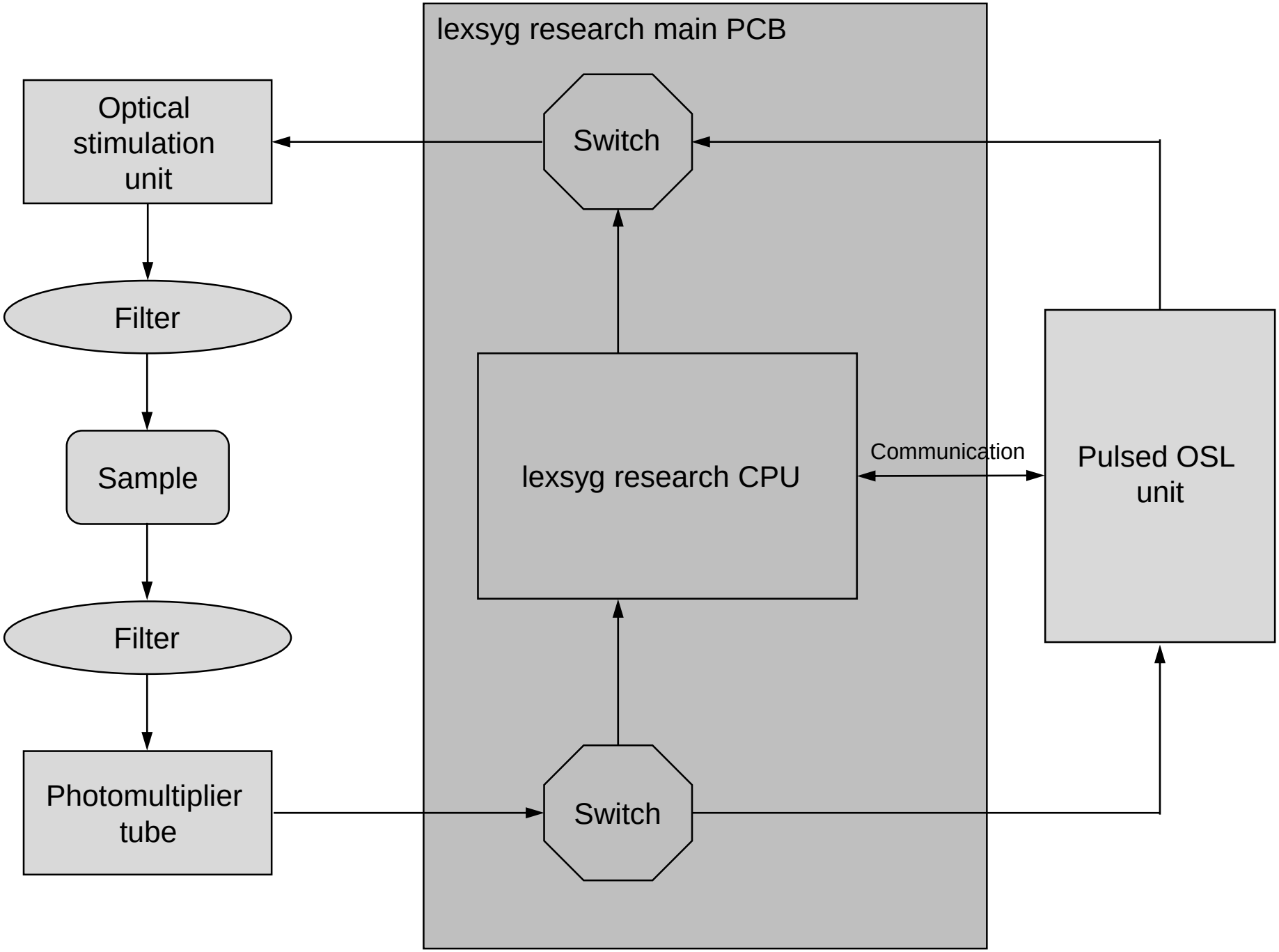
lexsyg research main PCB
Optical stimulation unit
Switch
Filter
Sample
Filter
Photomultiplier tube
lexsyg research CPU
Communication
Pulsed OSL unit
Switch

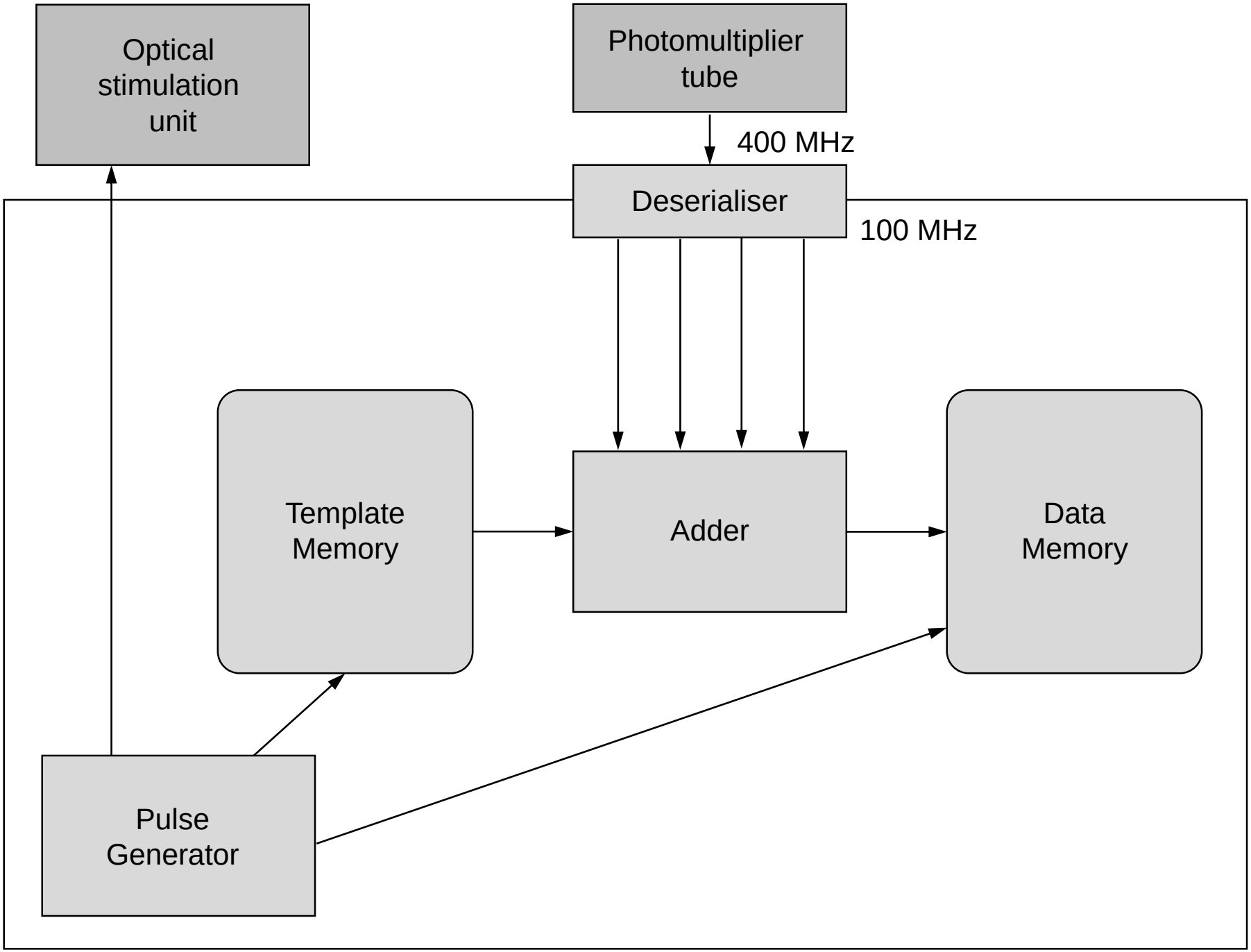
Optical stimulation unit
Photomultiplier tube
400 MHz
Deserialiser
100 MHz
Template Memory
Adder
Data Memory
Pulse Generator

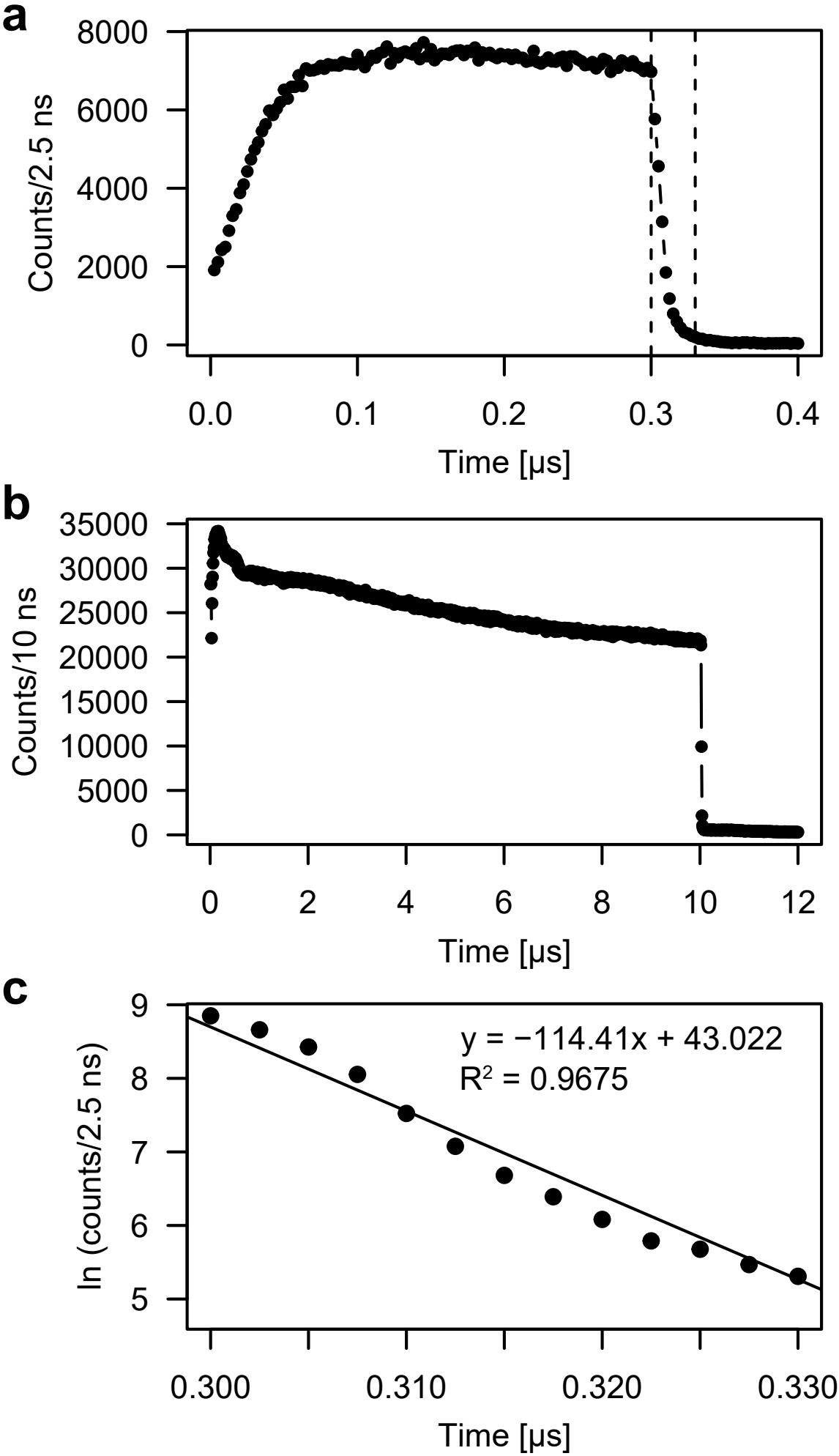
a
8000
6000
4000
2000
0
Counts/2.5 ns
0.0
0.1
0.2
0.3
0.4
Time [μs]
b
35000
30000
25000
20000
15000
10000
5000
0
Counts/10 ns
0
2
4
6
8
10
12
Time [μs]
c
9
8
7
6
5
ln (counts/2.5 ns)
y = −114.41x + 43.022
R2 = 0.9675
0.300
0.310
0.320
0.330
Time [μs]

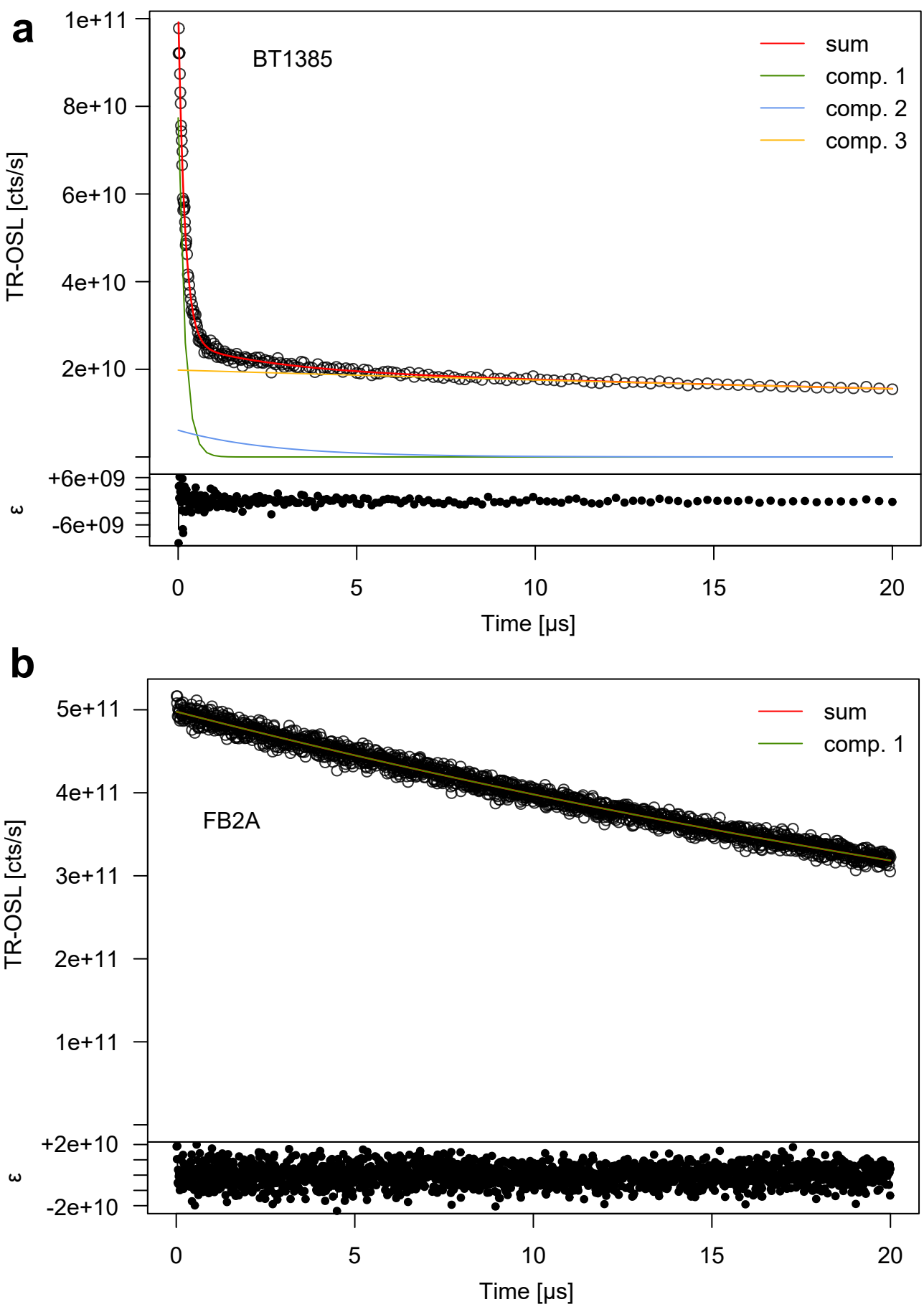
a
BT1385
sum
comp. 1
comp. 2
comp. 3
TR-OSL [cts/s]
1e+11
8e+10
6e+10
4e+10
2e+10
+6e+09
-6e+09
ε
0
5
10
15
20
Time [μs]
b
FB2A
sum
comp. 1
TR-OSL [cts/s]
5e+11
4e+11
3e+11
2e+11
1e+11
+2e+10
-2e+10
ε
0
5
10
15
20
Time [μs]

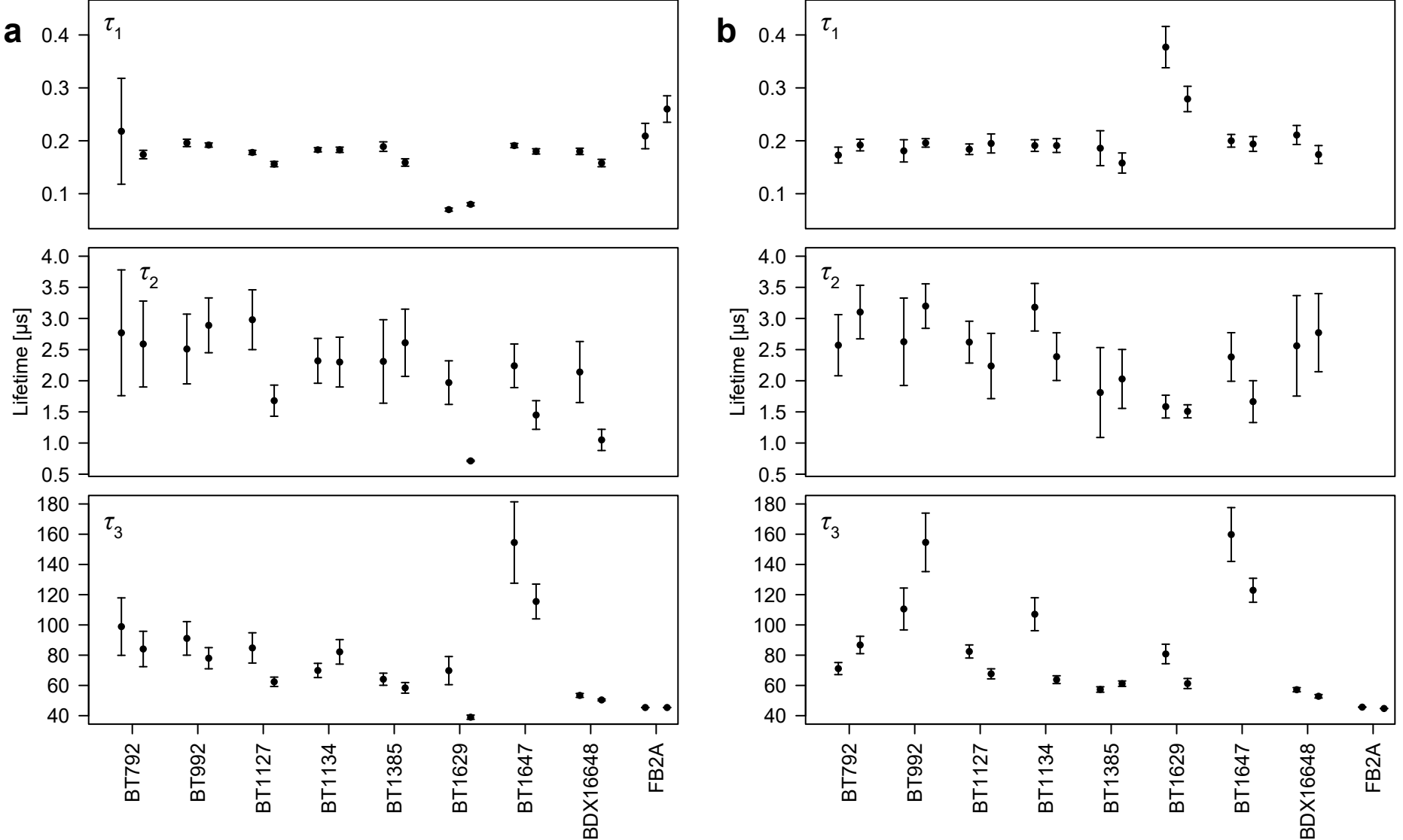
a
b
$\tau_1$
$\tau_2$
$\tau_3$
Lifetime [µs]
0.1
0.2
0.3
0.4
0.5
1.0
1.5
2.0
2.5
3.0
3.5
4.0
40
60
80
100
120
140
160
180
BT792
BT992
BT1127
BT1134
BT1385
BT1629
BT1647
BDX16648
FB2A

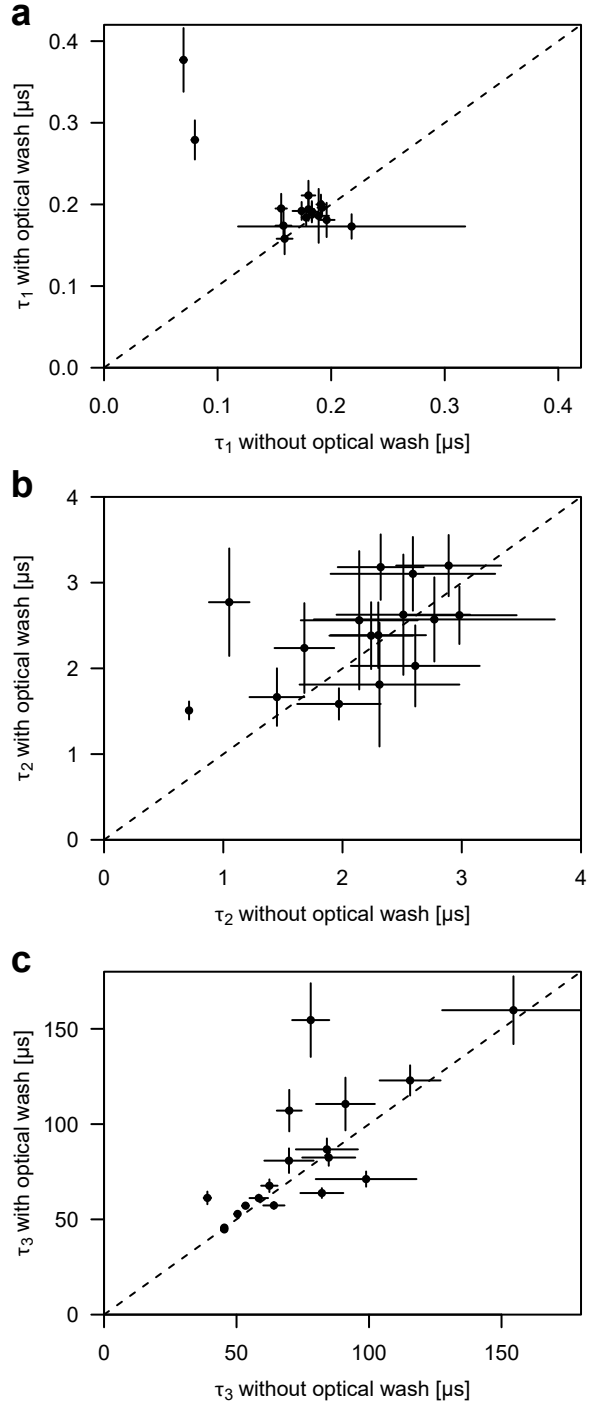
a
0.4
0.3
0.2
0.1
0.0
τ1 with optical wash [μs]
0.0
0.1
0.2
0.3
0.4
τ1 without optical wash [μs]
b
4
3
2
1
0
τ2 with optical wash [μs]
0
1
2
3
4
τ2 without optical wash [μs]
c
150
100
50
0
τ3 with optical wash [μs]
0
50
100
150
τ3 without optical wash [μs]

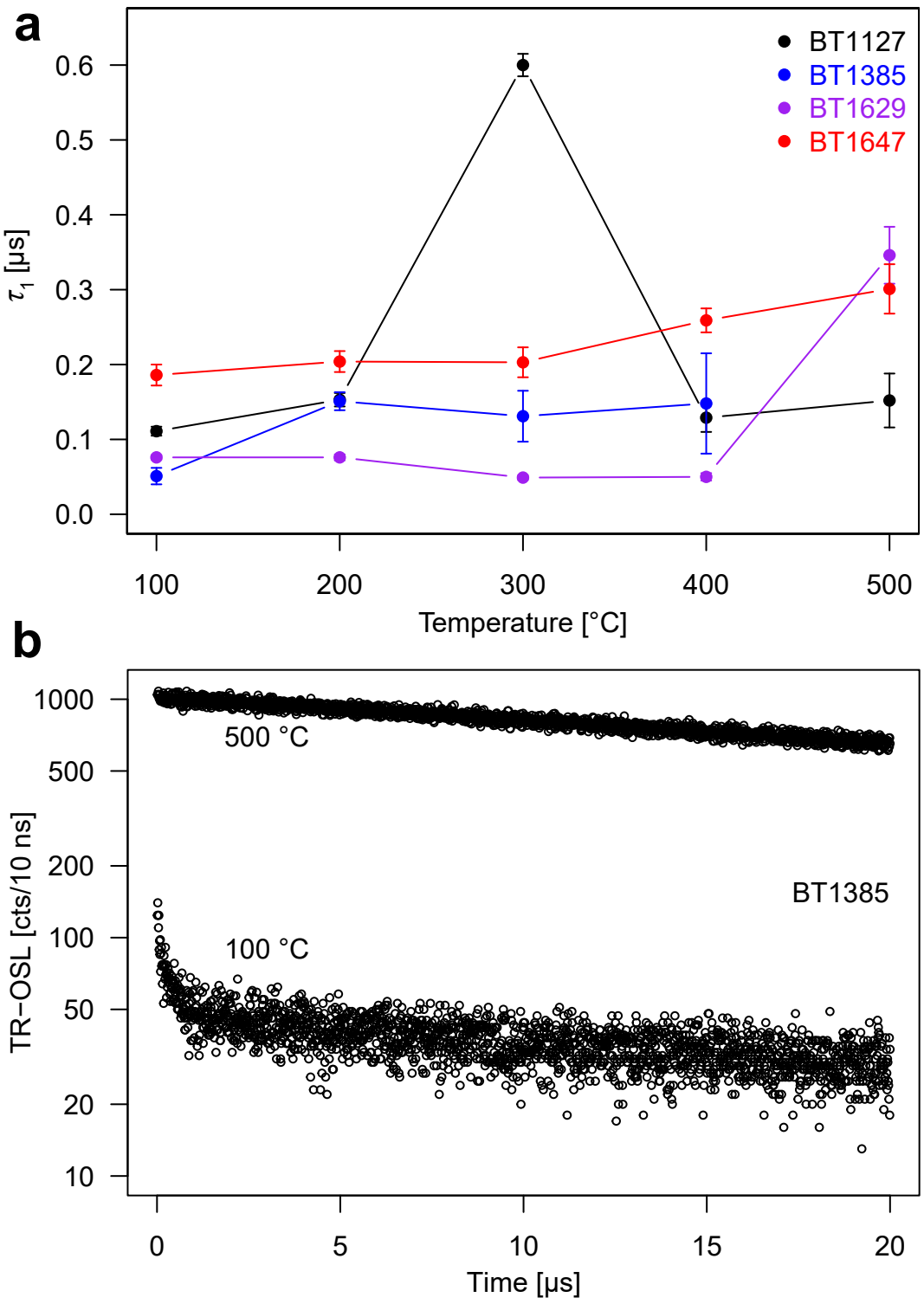
a
BT1127
BT1385
BT1629
BT1647
$\tau_1$ [µs]
0.0
0.1
0.2
0.3
0.4
0.5
0.6
100
200
300
400
500
Temperature [°C]
b
500 °C
BT1385
100 °C
TR−OSL [cts/10 ns]
10
20
50
100
200
500
1000
0
5
10
15
20
Time [µs]

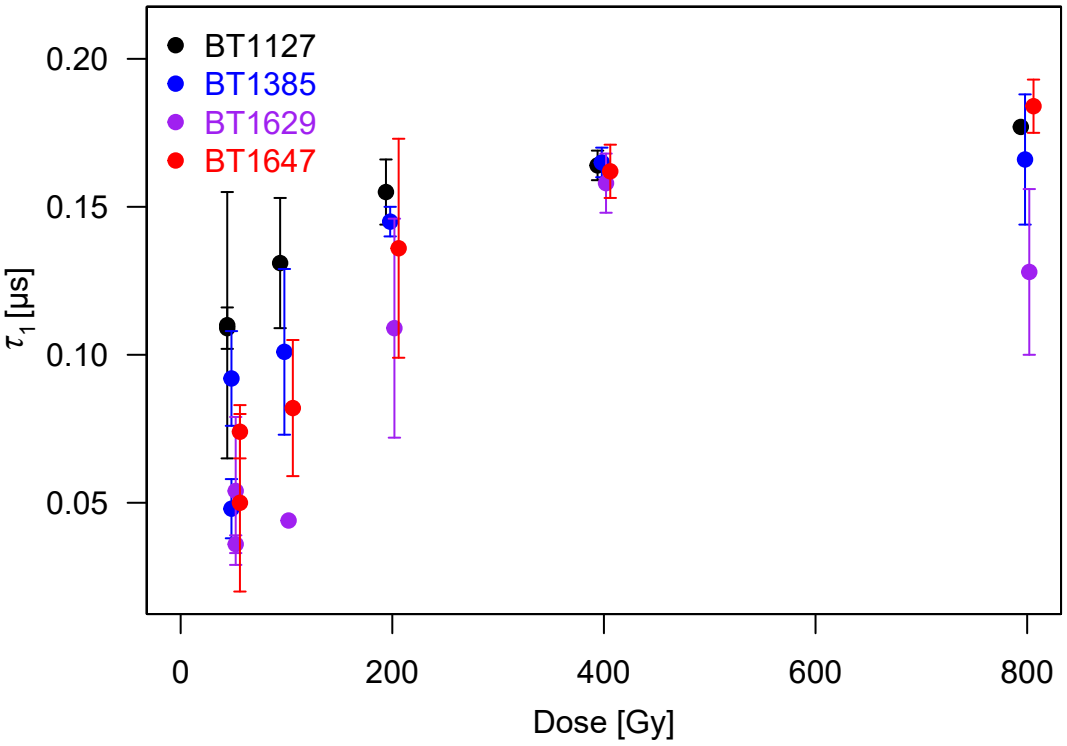
BT1127
BT1385
BT1629
BT1647
0.20
0.15
0.10
0.05
$\tau_1$ [µs]
0
200
400
600
800
Dose [Gy]

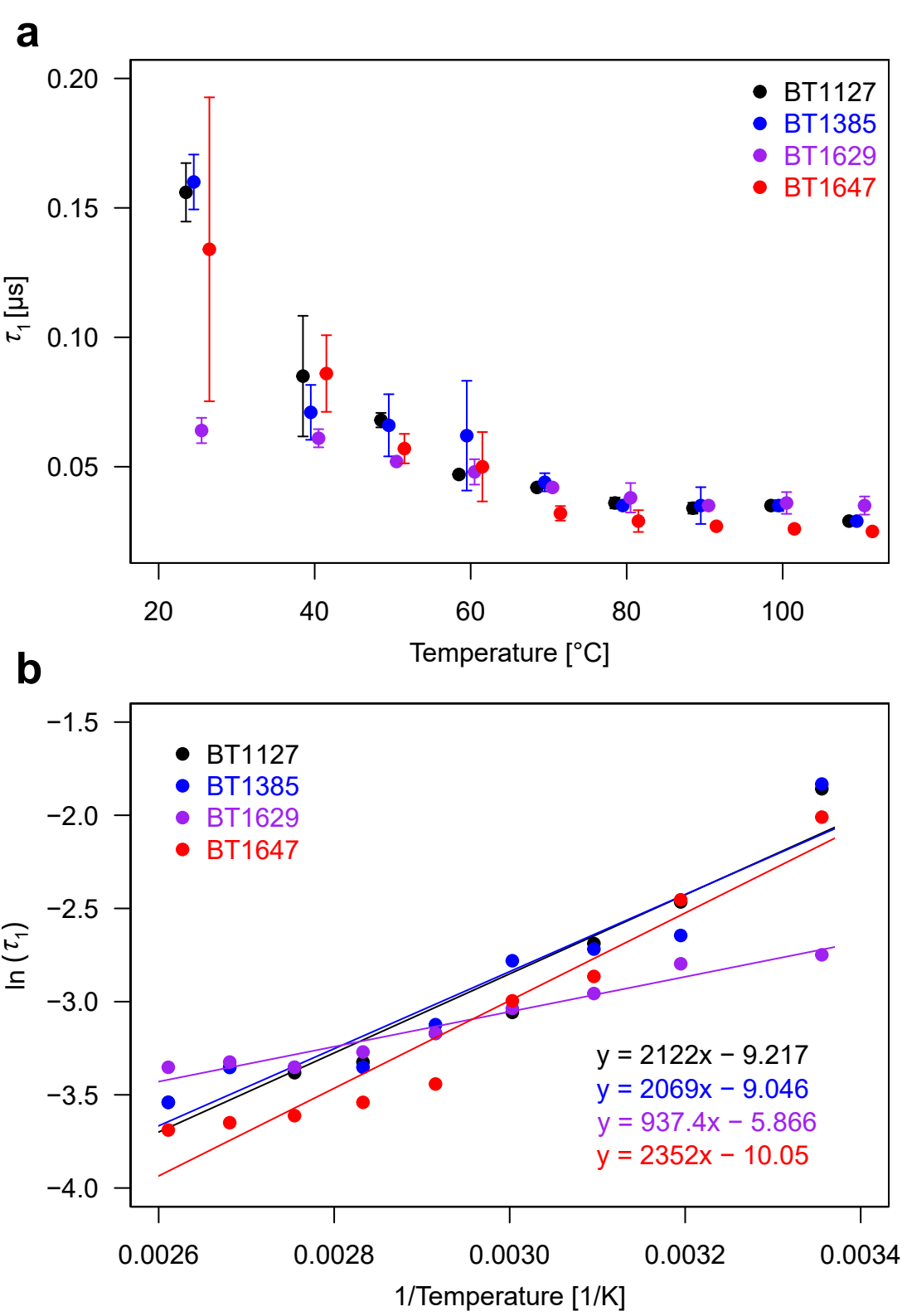
a
0.20
0.15
0.10
0.05
$\tau_1$ [µs]
BT1127
BT1385
BT1629
BT1647
20
40
60
80
100
Temperature [°C]
b
−1.5
−2.0
−2.5
−3.0
−3.5
−4.0
ln ($\tau_1$)
BT1127
BT1385
BT1629
BT1647
y = 2122x − 9.217
y = 2069x − 9.046
y = 937.4x − 5.866
y = 2352x − 10.05
0.0026
0.0028
0.0030
0.0032
0.0034
1/Temperature [1/K]

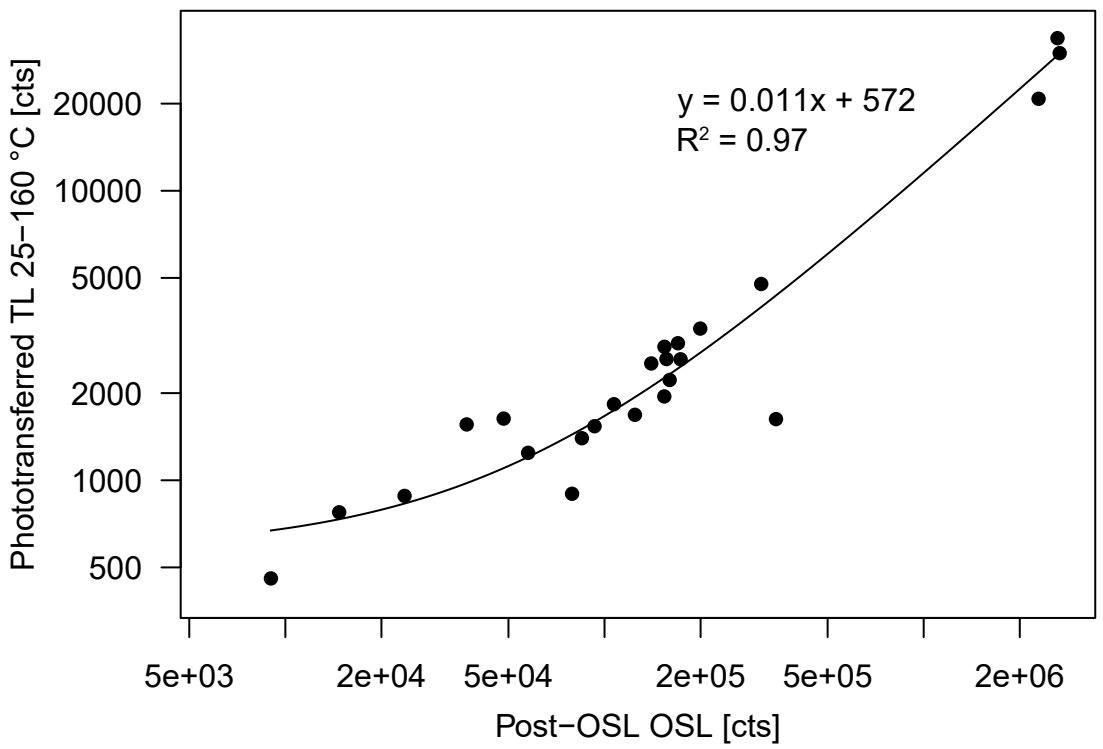
y = 0.011x + 572
R² = 0.97
Phototransferred TL 25−160 °C [cts]
20000
10000
5000
2000
1000
500
5e+03
2e+04
5e+04
2e+05
5e+05
2e+06
Post−OSL OSL [cts]

**Table 1** List of quartz samples used for the TR-OSL experiments.

| Laboratory code | Grain size [µm] | Origin | Reference |
|---|---|---|---|
| BT729 | 90–200 | Trebgast Valley, Germany | Unpublished |
| BT992 | 90–250 | Trebgast Valley, Germany | Unpublished |
| BT1127 | 90–200 | Trebgast Valley, Germany | Unpublished |
| BT1134 | 90–200 | Trebgast Valley, Germany | Kolb et al. [70] |
| BT1385 | 90–200 | Azraq, Jordan | Unpublished |
| BT1629 | 90–200 | Canaima, Venezuela (Roraima sandstone) | Unpublished |
| BT1647 | 90–200 | Weißenstadt, Germany (granite) | Unpublished |
| BDX16648 | 100–200 | Médoc, France | Kreutzer et al. [71] |
| FB2A | 150–250 | Fontainebleau, France | Kreutzer et al. [49] |

**Table 2** Summary of lifetimes obtained for the set of samples following a regenerative β-dose of 250 Gy and either no further optical pre-treatment ('without optical wash') or with an optical wash prior to TR-OSL measurement consisting of exposure to blue LDs (445 nm) at 160 °C for 100 s at a power density of 16 mW $cm^{-2}$. Two aliquots per sample were measured and the lifetimes were extracted using the fit_OSLLifeTimes() function of the **R** package 'Luminescence' (v0.9.0; upcoming version). Uncertainties are quoted at 1σ.

| | Without optical wash | | | With optical wash | | |
|---|---|---|---|---|---|---|
| | $\tau_1$ [μs] | $\tau_2$ [μs] | $\tau_3$ [μs] | $\tau_1$ [μs] | $\tau_2$ [μs] | $\tau_3$ [μs] |
| BT729 | 0.218 ± 0.100 | 2.77 ± 1.01 | 98.9 ± 19.0 | 0.173 ± 0.015 | 2.57 ± 0.49 | 71.1 ± 4.0 |
| | 0.174 ± 0.008 | 2.59 ± 0.69 | 84.1 ± 11.7 | 0.192 ± 0.011 | 3.10 ± 0.43 | 86.7 ± 5.7 |
| BT992 | 0.196 ± 0.007 | 2.51 ± 0.56 | 91.1 ± 11.1 | 0.181 ± 0.021 | 2.63 ± 0.70 | 111 ± 14 |
| | 0.192 ± 0.004 | 2.89 ± 0.44 | 78.0 ± 7.0 | 0.196 ± 0.008 | 3.20 ± 0.36 | 155 ± 19 |
| BT1127 | 0.178 ± 0.004 | 2.98 ± 0.48 | 84.8 ± 10.0 | 0.184 ± 0.010 | 2.62 ± 0.34 | 82.5 ± 4.3 |
| | 0.156 ± 0.005 | 1.68 ± 0.25 | 62.4 ± 3.1 | 0.195 ± 0.018 | 2.24 ± 0.52 | 67.7 ± 3.3 |
| BT1134 | 0.183 ± 0.004 | 2.32 ± 0.36 | 69.9 ± 4.7 | 0.191 ± 0.011 | 3.18 ± 0.38 | 107 ± 11 |
| | 0.183 ± 0.005 | 2.30 ± 0.40 | 82.2 ± 8.1 | 0.191 ± 0.013 | 2.39 ± 0.38 | 63.8 ± 2.6 |
| BT1385 | 0.189 ± 0.009 | 2.31 ± 0.67 | 64.1 ± 4.0 | 0.186 ± 0.033 | 1.81 ± 0.72 | 57.3 ± 1.8 |
| | 0.159 ± 0.007 | 2.61 ± 0.54 | 58.4 ± 3.5 | 0.158 ± 0.019 | 2.03 ± 0.47 | 61.2 ± 1.8 |
| BT1629 | 0.070 ± 0.003 | 1.97 ± 0.35 | 69.8 ± 9.3 | 0.377 ± 0.039 | 1.59 ± 0.18 | 80.8 ± 6.5 |
| | 0.080 ± 0.003 | 0.71 ± 0.01 | 39.0 ± 1.4 | 0.279 ± 0.024 | 1.51 ± 0.11 | 61.3 ± 3.3 |
| BT1647 | 0.191 ± 0.004 | 2.24 ± 0.35 | 155 ± 27 | 0.200 ± 0.012 | 2.38 ± 0.39 | 160 ± 18 |
| | 0.180 ± 0.005 | 1.45 ± 0.23 | 116 ± 12 | 0.194 ± 0.014 | 1.67 ± 0.34 | 123 ± 7.9 |
| BDX16648 | 0.180 ± 0.006 | 2.14 ± 0.49 | 53.4 ± 1.3 | 0.211 ± 0.018 | 2.56 ± 0.81 | 57.2 ± 1.4 |
| | 0.158 ± 0.007 | 1.05 ± 0.17 | 50.4 ± 0.6 | 0.174 ± 0.017 | 2.77 ± 0.63 | 52.8 ± 1.2 |
| FB2A | 0.209 ± 0.024 | NA | 45.4 ± 0.1 | NA | NA | 45.6 ± 0.2 |
| | 0.260 ± 0.025 | NA | 45.4 ± 0.1 | NA | NA | 44.8 ± 0.1 |

**Table 3** Sequence of measurements to record PTTL induced by the OSL slow component region.

| Step | Treatment | Purpose |
|---|---|---|
| 1 | Irradiation with 250 Gy β-dose | Give laboratory dose |
| 2 | Preheat at 220 °C for 10 s (5 K $s^{-1}$) | Remove charge from thermally unstable traps |
| 3 | OSL at 160 °C for 100 s (~16 mW $cm^{-2}$) | Remove fast and medium OSL components |
| 4 | OSL at RT for 1,000 s (~32 mW $cm^{-2}$) | Deplete the OSL slow component region ('Post-OSL OSL') |
| 5 | TL to 160 °C (5 K $s^{-1}$) | Measure PTTL induced by OSL slow components |